Chapter 5

Parameter space for resonant leptogenesis within the framework of minimal inverse seesaw model

We investigate the parameter space of the minimal inverse seesaw ISS(2,2) model for successful leptogenesis. The framework of ISS(2, 2) is realized by augmenting the Standard Model with two right-handed and two Standard Model gauge singlet neutrinos. The decay of the heavy sterile states which is essentially an admixture of the right-handed and SM singlet neutrino states produces the baryon asymmetry of the universe. In this predictive model of leptogenesis, we study resonant leptogenesis where the mass splitting between the heavy sterile states is naturally achieved. We review the possibility of generating the observed baryon asymmetry of the universe via leptogenesis where the CP violation comes solely from the low-energy CP phases. In addition, we investigate the effect of texture zero in the Dirac mass matrix on the model's parameter space for successful resonant leptogenesis.

5.1 Introduction

Despite the success of the Standard Model (SM) of particle physics, it fails to explain the observed tiny neutrino masses and the observed baryon asymmetry of the Universe (BAU). The remedy to such a limitation is the extension of the SM with extra sterile singlets like the seesaw models [1–5]. The type-I seesaw mechanism is the simplest extension of the SM, and the observed BAU can be explained via thermal leptogenesis in such an extension [6]. In such a scenario, the SM is extended by adding singlet right-handed (RH) neutrinos, and their out-of-equilibrium, lepton number violating decays cause lepton asymmetries, which are then processed in baryon asymmetries via sphaleron interactions [7].

Successful leptogenesis introduces a lower bound on the mass scales of the RH neutrino of about 10^9 GeV in the standard type-I seesaw with hierarchical RH neutrino mass spectrum [8]. However, if the RH neutrinos have a quasi-degenerate mass spectrum, the mass scale for successful leptogenesis may be reduced.

Another theoretically motivated extension of SM with low-scale sterile neutrinos is the inverse seesaw (ISS) mechanism, where two types of sterile neutrinos: RH neutrinos and SM gauge singlets, are introduced to the SM [9–14]. Due to the presence of a small lepton-number violating mass parameter, μ, the light neutrino mass is doubly suppressed allowing the Yukawa coupling to be much larger at the TeV scale of sterile neutrino mass. In addition to this, a feature of this model is that the quasi-degeneracy in the sterile neutrinos can be naturally realized due to the presence of a small lepton-number violating mass parameter [9, 10, 15–19]. As the mass parameter μ allows the sterile states to acquire a quasi-degenerate mass scale, resonantly enhanced leptogenesis can be naturally realized in such a model without fine-tuning. The ISS mechanism is a low-scale model making it testable in future experiments. In the context of baryogenesis, since the mass scale of the sterile neutrinos relevant to leptogenesis is low, one needs to consider a fully-flavored leptogenesis regime. In a low-scale leptogenesis, the low-energy CP-violating phases can related to the high-energy CP-violation necessary to produce the BAU.

Motivated by the fact that the measurements of the low-energy CP-phases are not as precise as the neutrino mixing angles in the neutrino oscillation experiments, we aim to study the effect of these phases on leptogenesis. We consider a minimal form of ISS mechanism that can accommodate the neutrino oscillation experimental data i.e., SM extended with two RH neutrinos and two sterile gauge singlets [11, 20–26]. We then proceed to find the parameter space of the defined model such that the BAU is generated effectively.

This chapter is organized as follows. In section 5.2, we describe the framework of the ISS(2, 2) model and define the three scenarios in which we study the implications of leptogenesis. In section 5.3, we review how resonant leptogenesis can be naturally achieved within the ISS(2, 2) framework. It also includes the results of our numerical analysis beginning with section 5.3.1 where we show the results of the parameter scan for the scenario where the R matrix has complex entries. Section 5.3.2 presents the results of the analysis for the case where R has a special form with real entries and the parameter space for the third scenario with texture zeros in Dirac mass matrix is presented in section 5.3.3. We finally summarize our conclusions in section 5.4.

5.2 Model Framework

We have considered the extension of SM by introducing two RH neutrinos and two SM gauge singlet fermions which results in a minimal form of ISS and is denoted by ISS(2,2). The Lagrangian of the model which is invariant under the SM gauge symmetry is,

$$-\mathcal{L}_\nu = Y_\nu \bar{l}_L \tilde{H} N_R + M_R \left(\bar{N}_R\right)^c (S_L)^c + \frac{1}{2}\mu \bar{S}_L (S_L)^c + h.c., \tag{5.1}$$

where $\bar{l}_L$ is the SM lepton doublet, $\tilde{H} = i\sigma_2 H^*$ with H being the SM Higgs doublet and σ denotes the 2^{nd} Pauli matrix. The extension of the SM includes the RH neutrinos N_R and the SM gauge singlets S_L. As the Higgs doublet H acquires vacuum expectation value (vev) and the gauge symmetry is broken i.e.,

$SU(2)_L \otimes U(1)_Y \to U(1)_{EM}$, we obtain the light neutrino mass matrix,

$$M_\nu = \begin{pmatrix} 0 & m_D & 0 \\ m_D^T & 0 & M_R \\ 0 & M_R^T & \mu \end{pmatrix}, \tag{5.2}$$

where $m_D = Y_\nu v$ represents the Dirac mass matrix, M_R is a complex 2×2 mass matrix and μ is a complex, symmetric 2×2 matrix. With $\mu \ll m_D \ll M_R$, diagonalization of equation (5.2) gives,

$$m_\nu = m_D \left(M_R^T\right)^{-1} \mu \left(M_R\right)^{-1} m_D^T. \tag{5.3}$$

As can be seen in equation (5.3), the light neutrinos are suppressed by the smallness of $\left(m_D M_R^{-1}\right)^2$ as well as the parameter μ. In the one-generation case, the masses of the light neutrinos can be reproduced for the following scale of the different mass states [10],

$$\left(\frac{m_\nu}{0.1 \text{ eV}}\right) = \left(\frac{m_D}{100 \text{ GeV}}\right)^2 \left(\frac{\mu}{1 \text{ keV}}\right) \left(\frac{M_R}{10^4 \text{ GeV}}\right)^{-2}, \tag{5.4}$$

The neutrino mass matrix of equation (5.3) can be approximately diagonalized by the unitary matrix U_{PMNS} as follows,

$$U_{\text{PMNS}}^\dagger m_\nu U_{\text{PMNS}}^* = \text{diag}(m_1,\ m_2,\ m_3) = m_d \tag{5.5}$$

where the unitary matrix in the standard parametrization is represented by,

$$U_{\text{PMNS}} = \begin{pmatrix} c_{12}c_{13} & s_{12}c_{13} & s_{13}e^{-i\delta} \\ -s_{12}c_{23} - c_{12}s_{23}s_{13}e^{i\delta} & c_{12}c_{23} - s_{12}s_{23}s_{13}e^{i\delta} & s_{23}c_{13} \\ s_{12}s_{23} - c_{12}c_{23}s_{13}e^{i\delta} & -c_{12}s_{23} - s_{12}c_{23}s_{13}e^{i\delta} & c_{23}c_{13} \end{pmatrix} \cdot P \tag{5.6}$$

with $P = \text{diag}(1,\ e^{i\alpha_{21}/2},\ e^{i\alpha_{31}/2})$, $s_{ij} = \sin\theta_{ij}$ and $c_{ij} = \cos\theta_{ij}$, δ is the Dirac CP phase and α_{21}, α_{31} are the Majorana phases.

A salient feature of the ISS(2,2) model is that one of the three light neutrinos is massless and thus one of the Majorana CP phases becomes unphysical. To be more specific, for the case of normal hierarchy (NH) we have $m_1 = 0 < m_2 < m_3$ with the single Majorana phase redefined as $\sigma = (\alpha_{21} - \alpha_{31})/2$ and $m_3 = 0 < m_1 < m_2$ for inverted hierarchy (IH) with the single Majorana phase given as $\sigma = \alpha_{21}/2$.

Using equations (5.3) and (5.5), we can derive the Casas-Ibarra [27] type parametrization of the Dirac mass matrix for the inverse seesaw model as [28],

$$\left(m_d^{-1/2} U_{\text{PMNS}}^{\dagger} m_D \left(M_R^T\right)^{-1} \mu^{1/2}\right) \cdot \left(\mu^{1/2} M_R^{-1} m_D^T U_{\text{PMNS}}^{*} m_d^{-1/2}\right) = I, \tag{5.7}$$

which leads to,

$$m_D = U_{\text{PMNS}}\; m_d^{1/2}\; R\; \mu^{-1/2}\; M_R^T \tag{5.8}$$

where R is a complex 3×2 matrix given by,

$$R = \begin{pmatrix} 0 & 0 \\ \cos\zeta & -\sin\zeta \\ \sin\zeta & \cos\zeta \end{pmatrix} \qquad \text{for NH} \tag{5.9}$$

$$\text{and, } R = \begin{pmatrix} \cos\zeta & -\sin\zeta \\ \sin\zeta & \cos\zeta \\ 0 & 0 \end{pmatrix} \qquad \text{for IH} \tag{5.10}$$

with $z = Re(\zeta) + i\ Im(\zeta)$, being a complex parameter in general. In the next section of this chapter, we analyze the parameter space for successful resonant leptogenesis for three different scenarios in the ISS(2, 2) model, namely, (i) R matrix with complex ζ: here the source of CP-violation comes from the matrix R and the CP-phases present in the PMNS matrix, (ii) R matrix with $Re(\zeta) = \pi/4$ and $Im(\zeta) = 0$: in such a special case CP-violation necessary for leptogenesis comes from the Dirac and Majorana CP-phases, and (iii) texture zeros in m_D: in this scenario we consider one of the elements of m_D to be zero such that we can write the parameter ζ in terms of the neutrino mass, mixing angles and the CP-phases of the U_{PMNS} matrix. Thus, just as in scenario (ii), the CP-phases present in the PMNS matrix provide the necessary CP-violation.

5.3 Resonant Leptogenesis in ISS(2, 2) Model

To study leptogenesis in the ISS(2,2) model, we work in the basis where the sterile neutrino mass sub-matrix is real and diagonal. The lower 2×2 block of the mass matrix presented in the equation (5.2) is given as

$$M_{SN} = \begin{pmatrix} 0 & M_R \\ M_R^T & \mu \end{pmatrix} \tag{5.11}$$

We perform a block diagonalization on the above matrix such that we are working in the basis where the sterile neutrinos are in their mass basis. This transforms the mass matrix given in the equation (5.2) by rotating the Yukawa couplings to the SM leptons and can be written as

$$M_\nu \to M_\nu \simeq \begin{pmatrix} 0 & m_D^{'} & 0 \\ \left(m_D^{'}\right)^T & M_R - \frac{1}{2}\mu & 0 \\ 0 & 0 & M_R + \frac{1}{2}\mu \end{pmatrix}, \tag{5.12}$$

where $m_D^{'}$ is the rotated Yukawa coupling matrix. It is clear from the equation (5.12) that for small values of μ the mass spectrum of the heavy sterile neutrinos becomes almost degenerate and the scenario of resonant leptogenesis can be naturally achieved. In resonant leptogenesis, the CP-violating, out-of-equilibrium decay of the degenerate sterile neutrinos produces the observed BAU. A non-zero lepton asymmetry is generated from the CP-violation obtained from the interference of the tree-level decay of the sterile neutrinos with the one-loop level. In the case of quasi-degenerate sterile neutrinos, the self-energy correction is resonantly enhanced and the flavor-dependent CP asymmetry is defined as [29–31]

$$\varepsilon_i^\alpha = \frac{\Gamma\left(N_{i\alpha} \to l_\alpha \Phi\right) - \Gamma\left(N_{i\alpha} \to l_\alpha^c \Phi^\dagger\right)}{\sum_\alpha \left[\Gamma\left(N_{i\alpha} \to l_\alpha \Phi\right) + \Gamma\left(N_{i\alpha} \to l_\alpha^c \Phi^\dagger\right)\right]} \tag{5.13}$$

The CP-asymmetry parameters are given by

$$\varepsilon_i^\alpha = \sum_{i \neq j} \frac{\mathrm{Im}\left[h_{i\alpha}^\dagger h_{\alpha j}\left(h^\dagger h\right)_{ij}\right] + \frac{M_i}{M_j}\mathrm{Im}\left[h_{i\alpha}^\dagger h_{\alpha j}\left(h^\dagger h\right)_{ji}\right]}{\left(h^\dagger h\right)_{ii}\left(h^\dagger h\right)_{jj}} \cdot \frac{\left(M_i^2 - M_j^2\right) \cdot M_i \Gamma_j}{\left(M_i^2 - M_j^2\right)^2 + M_i^2 \Gamma_j^2}. \tag{5.14}$$

where, $h = \frac{\sqrt{2}}{v} m'_D$, Γ_i is the decay width of the heavy sterile neutrino state N_i, and M_i is the mass eigenvalue of N_i. A lepton asymmetry is generated by utilizing the above CP-asymmetry parameter by solving the Boltzmann equation (5.15). The Boltzmann equation under consideration is a coupled differential equation describing the time evolution of the density of heavy sterile neutrinos, n_{N_i}, and the lepton number density $n_{N_{\alpha\alpha}}$ (with $\alpha = e, \mu, \tau$) [32],

$$\begin{aligned} \frac{dn_{N_i}}{dz} &= -D_i \left(n_{N_i} - n_{N_i}^{eq} \right) \\ \frac{n_{N_{\alpha\alpha}}}{dz} &= \sum_{i=1}^{2} \varepsilon_i^{\alpha} D_i \left(n_{N_i} - n_{N_i}^{eq} \right) - W_{ID}\, n_{N_{\alpha\alpha}} \end{aligned} \tag{5.15}$$

where

$$W_{ID} = \frac{1}{4} K z^3 \mathcal{K}_1(z), \tag{5.16}$$

$$D_i = \frac{z}{H(z=1)} \cdot \frac{\Gamma_i}{n_{N_i}^{eq}}, \tag{5.17}$$

denotes the washout due to inverse decay and the decay term, respectively, with $\mathcal{K}_1(z)$ being the modified Bessel function of the first kind, the parameter H is the Hubble parameter, $\tilde{m}$ is the effective neutrino mass, and m_* is the equilibrium neutrino mass, $K = \tilde{m}/m_*$ is known as the decay parameter, $n_{N_i}^{eq}$ is the equilibrium number density of N_i and is defined as

$$n_{N_i}^{eq} = \frac{3}{8} z^2 \mathcal{K}_2(z) \tag{5.18}$$

where, $z = \frac{M_{R_1}}{T}$ and $\mathcal{K}_2$ is the modified Bessel function of the second kind.

The baryon asymmetry, η_B can be estimated by solving equations (5.15), and the value of η_B depends on the initial condition of the heavy sterile neutrinos. The numerical evaluation of baryon asymmetry performed in this work involves the decay of sterile neutrinos which is a good approximation, and we do not consider other effects such as the scattering process, spectator effects, thermal corrections, etc. In our analysis, we choose M_R and μ matrices to be diagonal with a degenerate mass spectrum of right-handed neutrinos, $M_{R_1} = M_{R_2} = 1$ TeV. The elements of the matrix μ determine the level of degeneracy among the heavy sterile states and we take μ_i to be free parameters that will be constrained by successful leptogenesis.

Further, we choose a vanishing initial abundance of sterile neutrinos and scan over the parameters of our model, namely: $\delta,\ \sigma,\ \mu_1,\ \mu_2,\ Re(\zeta),\ Im(\zeta)$. We make a parameter scan by using flat prior and define 1σ, 2σ, and 3σ regions of agreement with the observed value of baryon asymmetry by evaluating the log-likelihood function at a point, p. The function is given as

$$log\ L = -\frac{1}{2}\left(\frac{\eta_B^2(p) - \eta^2_{B_{CMB}}}{\Delta\eta^2_{B_{CMB}}}\right) \tag{5.19}$$

Depending on the scenarios discussed in section (5.2), we will have different dimensions of p.

5.3.1 Scenario I: R matrix with complex ζ

This analysis examines the most general scenario within a six-dimensional parameter space, denoted by $p = (\delta, \sigma, \mu_1,\ \mu_2,\ Re(\zeta),\ Im(\zeta))$, using the `MultiNest` package [33]. The investigation involves a comprehensive scan across this parameter space. The results of our analysis, displayed in Figure 5.1, present a 2D projection that includes resonant leptogenesis incorporating CP-violating effects from the complex matrix R, alongside the phases of the PMNS matrix. The mass splitting between the two sterile states, which is necessary for successful resonant leptogenesis is quantified by the parameters μ_1, and μ_2. Figure 5.1 illustrates the variation in the baryon asymmetry, η_B, within the $(\mu_1 - \mu_2)$ parameter space. The derived best-fit values for the model's free parameter, within the normal hierarchy (NH), are $\delta = 194°$, $\sigma = 152°$, $\log_{10}(\mu_1/\text{GeV}) = -3.6$, $\log_{10}(\mu_2/\text{GeV}) = -3.0$, $Re(\zeta) = 154°$, and $Im(\zeta) = 193°$. Notably, the measured δ aligns with the global fit of experimental data reported in NuFit 5.1 [34] for the NH. Conversely, for the inverted hierarchy (IH), the best–fit values are $\delta = 203°$, $\sigma = 216°$, $\log_{10}(\mu_1/\text{GeV}) = -2.9$, $\log_{10}(\mu_2/\text{GeV}) = -2.8$, $Re(\zeta) = 175°$, and $Im(\zeta) = 212°$. However, in the IH case, the measured δ lies beyond the 1σ range of the global neutrino oscillation experimental data. For the range of δ between $[92 - 296]°$ we obtain the 1σ value of the observed baryon asymmetry, η_B in the NH case and $[117 - 289]°$ in the IH case.

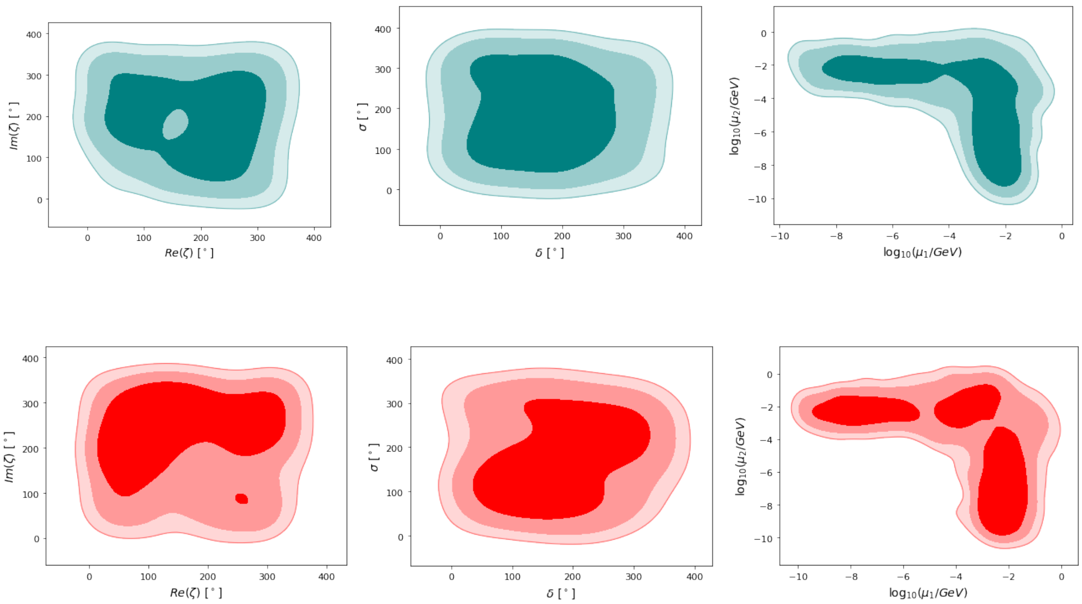

Figure 5.1: The projection for leptogenesis with the contours representing the 1σ, 2σ, and 3σ confidence levels. The teal and red colour denotes the case of NH and IH, respectively.

5.3.2 Scenario II: R is a real matrix with $Re(\zeta) = \pi/4$ and $Im(\zeta) = 0$

For the second case, we choose $Re(\zeta) = \pi/4$ and $Im(\zeta) = 0$ making the R matrix real such that the necessary CP violation comes solely from the CP phases present in the neutrino mixing matrix. It is clear that the generation of BAU has a contribution from high as well as low energy parameters, however, in this case, we analyze the effect of low-energy CP phases on leptogenesis in the ISS(2,2) model. We first make a parameter scan in a 4-dimensional parameter space with $p = (\delta,\ \sigma,\ \mu_1,\ \mu_2)$. Figure 5.2 shows the allowed region for the parameters of the model. The contours represent the region for which the observed value of baryon asymmetry can be obtained within 1σ, 2σ, and 3σ confidence intervals. The best-fit values for the parameters are $\delta = 167°$, $\sigma = 216°$, $\log_{10}(\mu_1/\text{GeV}) = -4.0$, $\log_{10}(\mu_2/\text{GeV}) = -3.9$ in the NH case. For the IH case, the best-fit values are $\delta = 241°$, $\sigma = 109°$, $\log_{10}(\mu_1/\text{GeV}) = -4.2$, $\log_{10}(\mu_2/\text{GeV}) = -3.5$. For the range

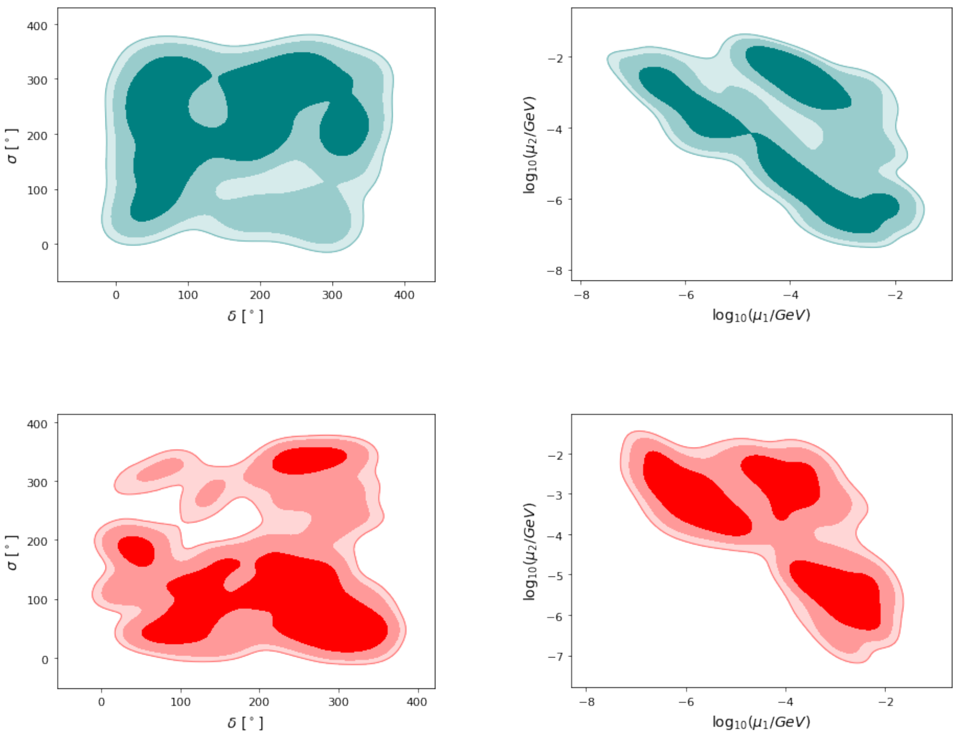

Figure 5.2: The projection for leptogenesis with the contours representing the 1σ, 2σ, and 3σ confidence levels. The teal and red colour denotes the case of NH and IH, respectively.

of δ between $[46-288]^\circ$ we obtain the 1σ value of the observed baryon asymmetry, η_B in the NH case and $[140-342]^\circ$ in the IH case. We find that the value of δ calculated within the model that obtains the best-fit value of the observed BAU lies within the 1σ region of NuFit 5.1 data for the case of NH, however, it lies slightly outside the 1σ range for the IH case.

5.3.3 Scenario III: texture zeros in m_D

We consider one of the elements of the Yukawa matrix, m_D to be zero. Considering the (1, 1) element of m_D to be zero we obtain a simple expression using Casas-Ibarra type parametrization of equation (5.8)

$$(U_{\rm PMNS})_{21}\sqrt{m_2}\cos\zeta + (U_{\rm PMNS})_{23}\sqrt{m_3}\sin\zeta = 0, \tag{5.20}$$

in the NH case, and,

$$(U_{\rm PMNS})_{11}\sqrt{m_1}\cos\zeta + (U_{\rm PMNS})_{22}\sqrt{m_2}\sin\zeta = 0, \tag{5.21}$$

in the IH case.

From the above relations, one can write the parameter ζ in terms of the neutrino masses, mixing angles, and the CP phases of the PMNS matrix. We have a 4-dimensional parameter space with a particular point defined as $p = (\delta,\ \sigma,\ \mu_1,\ \mu_2)$. The results of the exploration are presented in figure 5.3. The contours represent the region of the parameter space for which the observed value of baryon asymmetry lies within 1σ, 2σ, and 3σ confidence intervals. For the parameters of the model the best-fit value are $\delta = 196°$, $\sigma = 192°$, $\log_{10}(\mu_1/\text{GeV}) = -4.1$, $\log_{10}(\mu_2/\text{GeV}) = -3.9$ in the NH case. For the IH case, the best-fit values are $\delta = 204°$, $\sigma = 182°$, $\log_{10}(\mu_1/\text{GeV}) = -3.9$, $\log_{10}(\mu_2/\text{GeV}) = -3.4$. For the range of δ between $[86 - 306]°$ we obtain the 1σ value of the observed baryon asymmetry, η_B in the NH case and $[90 - 318]°$ in the IH case. From the best-fit values of the Dirac CP phase δ, we see that for both the NH as well as the IH cases the measured value agrees with the experimental data up to 1σ confidence level.

5.4 Conclusions

In this chapter, we have studied resonant leptogenesis in the framework of the minimal form of the inverse seesaw model ISS(2, 2). Here, the SM is extended by adding two right-handed and two SM gauge singlet neutrinos. Considering the quasi-degenerate, quasi-Dirac sterile neutrino states, we study the scenario of resonant leptogenesis.

To carry out our analysis, we write the Dirac mass matrix of the ISS(2, 2) model in the form of Casas-Ibarra type parametrization. We investigate the viable parameter space for resonant leptogenesis in the ISS(2, 2) model. We explored the parameter space for three different scenarios. Firstly, we consider the case where the CP violation necessary for successful leptogenesis comes from both

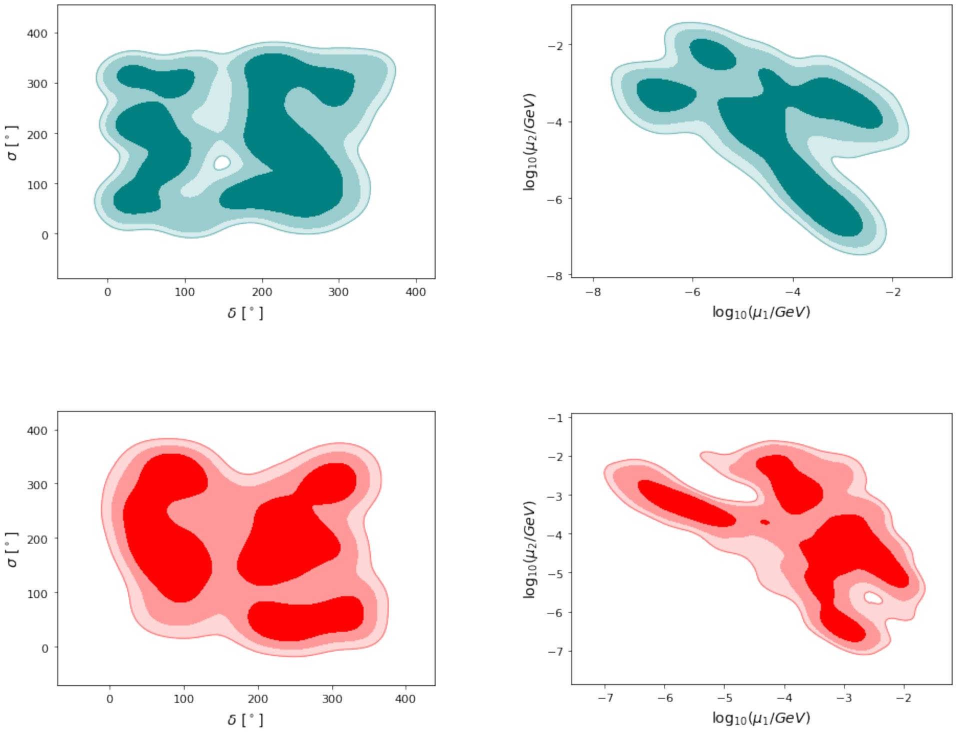

Figure 5.3: The projection for leptogenesis with the contours representing the 1σ, 2σ, and 3σ confidence levels. The teal and red colour denotes the case of NH and IH, respectively.

high-energy parameters (in the form of complex R matrix) and low-energy CP phases. Secondly, we assess the possibility of CP violation arising exclusively from the low-energy leptonic sector in the form of CP phases present in the PMNS matrix. Finally, the third case involves texture zero in the Dirac mass matrix which allows us to write the elements of the complex R matrix in terms of low-energy parameters. In other words, we explore the possibility of successful low-energy resonant leptogenesis with CP violation coming from the phases present in the PMNS matrix.

We take the best-fit values of the three mixing angles and two mass-squared differences as the input for the Casas-Ibarra parametrization and allow the complex parameter, ζ, the elements of the matrix μ and the two CP phases present in the PMNS matrix to run freely in a particular region as free parameters. We numerically solve the coupled Boltzmann equation that describes the evolution of the Lepton asymmetry and eventually gives the baryon asymmetry. We make a parameter exploration for the free parameters of the model using the measured value of baryon asymmetry. From the measured value of δ, we find that the model agrees with the experimental data of the Dirac CP phase up to 1σ confidence level in the NH case for all three scenarios, however, in the IH case it only agrees with the scenario where we consider texture zeros in the Dirac mass matrix. Future precision experiments may give more stringent results on the Dirac CP phase and probe such a model.

Bibliography

[1] Minkowski, P. $\mu\rightarrow$ eγ at a rate of one out of 109 muon decays? *Physics Letters B* **67** (4), 421–428, 1977.

[2] Mohapatra, R. N. & Senjanović, G. Neutrino mass and spontaneous parity nonconservation. *Physical Review Letters* **44** (14), 912, 1980.

[3] Yanagida, T. Horizontal symmetry and masses of neutrinos. *Progress of Theoretical Physics* **64** (3), 1103–1105, 1980.

[4] Gell-Mann, M. *et al.* Complex spinors and unified theories. In *Murray Gell-Mann: Selected Papers*, 266–272, World Scientific, 2010.

[5] Glashow, S. The future of elementary particle physics. In *Quarks and Leptons: Cargèse 1979*, 687–713, Springer, 1980.

[6] Fukugita, M. & Yanagida, T. Barygenesis without grand unification. *Physics Letters B* **174** (1), 45–47, 1986.

[7] Kuzmin, V. A. *et al.* On anomalous electroweak baryon-number non-conservation in the early universe. *Physics Letters B* **155** (1-2), 36–42, 1985.

[8] Davidson, S. & Ibarra, A. A lower bound on the right-handed neutrino mass from leptogenesis. *Physics Letters B* **535** (1-4), 25–32, 2002.

[9] González-Garciá, M. C. *et al.* Isosinglet-neutral heavy-lepton production in Z-decays and neutrino mass. *Nuclear Physics B* **342** (1), 108–126, 1990.

[10] Deppisch, F. & Valle, J. Enhanced lepton flavor violation in the supersymmetric inverse seesaw model. *Physical Review D* **72** (3), 036001, 2005.

[11] Abada, A. & Lucente, M. Looking for the minimal inverse seesaw realisation. *Nuclear Physics B* **885**, 651–678, 2014.

[12] Arina, C. *et al.* Minimal supergravity scalar neutrino dark matter and inverse seesaw neutrino masses. *Physical review letters* **101** (16), 161802, 2008.

[13] Dev, P. B. & Mohapatra, R. TeV scale inverse seesaw model in SO(10) and leptonic nonunitarity effects. *Physical Review D* **81** (1), 013001, 2010.

[14] Mukherjee, A. & Saha, A. K. Rescuing leptogenesis parameter space of inverse seesaw, 2023. 2307.14405.

[15] Wyler, D. & Wolfenstein, L. Massless Neutrinos in Left-Right Symmetric Models. *Nuclear Physics B* **218**, 205–214, 1983.

[16] Mohapatra, R. N. Mechanism for understanding small neutrino mass in superstring theories. *Physical Review Letters* **56** (6), 561, 1986.

[17] Mohapatra, R. N. & Valle, J. W. Neutrino mass and baryon-number nonconservation in superstring models. *Physical Review D* **34** (5), 1642, 1986.

[18] Ma, E. Lepton-number nonconservation in E_6 superstring models. *Physics Letters B* **191** (3), 287–289, 1987.

[19] González-Garciá, M. C. & Valle, J. W. Fast decaying neutrinos and observable flavour violation in a new class of majoron models. *Physics Letters B* **216** (3-4), 360–366, 1989.

[20] Malinskỳ, M. *et al.* Non-unitary neutrino mixing and CP violation in the minimal inverse seesaw model. *Physics Letters B* **679** (3), 242–248, 2009.

[21] Hirsch, M. *et al.* Minimal supersymmetric inverse seesaw: neutrino masses, lepton flavour violation and lhc phenomenology. *Journal of High Energy Physics* **2010** (1), 1–21, 2010.

[22] Blanchet, S. *et al.* Leptogenesis with TeV-scale inverse seesaw model in SO (10). *Physical Review D* **82** (11), 115025, 2010.

[23] Dias, A. G. *et al.* Simple realization of the inverse seesaw mechanism. *Physical Review D* **86** (3), 035007, 2012.

[24] Agashe, K. *et al.* Natural seesaw and leptogenesis from hybrid of high-scale type-I and TeV-scale inverse. *Journal of High Energy Physics* **2019** (4), 1–76, 2019.

[25] Abada, A. *et al.* Neutrino masses, leptogenesis and dark matter from small lepton number violation? *Journal of Cosmology and Astroparticle Physics* **2017** (12), 024–024, 2017.

[26] Fernández-Martínez, E. *et al.* HNL mass degeneracy: implications for low-scale seesaws, LNV at colliders and leptogenesis. *Journal of High Energy Physics* **2023** (3), 2023.

[27] Casas, J. & Ibarra, A. Oscillating neutrinos and $\mu \rightarrow$ e, γ. *Nuclear Physics B* **618** (1-2), 171–204, 2001.

[28] Dolan, M. J. *et al.* Dirac-phase thermal leptogenesis in the extended type-I seesaw model. *Journal of Cosmology and Astroparticle Physics* **2018** (06), 012, 2018.

[29] Pilaftsis, A. CP violation and baryogenesis due to heavy majorana neutrinos. *Physical Review D* **56** (9), 5431, 1997.

[30] Anisimov, A. *et al.* The CP-asymmetry in resonant leptogenesis. *Nuclear Physics B* **737** (1-2), 176–189, 2006.

[31] De Simone, A. & Riotto, A. On resonant leptogenesis. *Journal of Cosmology and Astroparticle Physics* **2007** (08), 013, 2007.

[32] De Simone, A. & Riotto, A. Quantum Boltzmann equations and leptogenesis. *Journal of Cosmology and Astroparticle Physics* **2007** (08), 002, 2007.

[33] Feroz, F. *et al.* MultiNest: an efficient and robust bayesian inference tool for cosmology and particle physics. *Monthly Notices of the Royal Astronomical Society* **398** (4), 1601–1614, 2009.

[34] Esteban, I. *et al.* The fate of hints: updated global analysis of three-flavor neutrino oscillations. *Journal of High Energy Physics* **2020** (9), 1–22, 2020.